

AperTO - Archivio Istituzionale Open Access dell'Università di Torino

Local structure of Cu(I) ions in the MOR zeolite: A DFT-assisted XAS study

This is the author's manuscript

Original Citation:

Availability:

This version is available <http://hdl.handle.net/2318/1768495> since 2021-01-22T18:27:57Z

Published version:

DOI:10.1016/j.radphyschem.2018.12.031

Terms of use:

Open Access

Anyone can freely access the full text of works made available as "Open Access". Works made available under a Creative Commons license can be used according to the terms and conditions of said license. Use of all other works requires consent of the right holder (author or publisher) if not exempted from copyright protection by the applicable law.

(Article begins on next page)

This is the author's final version of the contribution published as:

Buono C.; Martini A.; Pankin I.A.; Pappas D.K.; Negri C.; Kvande K.; Lomachenko K.A.; Borfecchia E., Local structure of Cu(I) ions in the MOR zeolite: A DFT-assisted XAS study. *Rad. Phys. Chem.*, 175, 2020, 108111.

DOI: 10.1016/j.radphyschem.2018.12.031

The publisher's version is available at:

<https://www.sciencedirect.com/science/article/pii/S0969806X18309289>

When citing, please refer to the published version.

Link to this full text:

<http://hdl.handle.net/2318/1768495>

Local structure of Cu(I) ions in the MOR zeolite: a DFT-assisted XAS study

C. Buono¹, A. Martini^{2,3}, I. A. Pankin^{2,3}, D. K. Pappas¹, C. Negri², K. Kvande¹, K. A. Lomachenko⁴, E. Borfecchia^{1,2,5*}

¹Center for Materials Science and Nanotechnology (SMN), Department of Chemistry, University of Oslo, 0315 Oslo (Norway)

²Department of Chemistry and INSTM Reference Center, University of Turin, 10125 Turin (Italy)

³International Research Institute “Smart Materials”, Southern Federal University, 344090 Rostov-on-Don (Russia)

⁴European Synchrotron Radiation Facility (ESRF), 38043 Grenoble Cedex 9 (France)

⁵Haldor Topsøe A/S, 2800 Kongens Lyngby (Denmark)

*e-mail: elisa.borfecchia@smn.uio.no

Abstract

We combine *in situ* XAS and DFT to determine the local structure of Cu(I) ions in the Cu-exchanged mordenite (MOR) zeolite, one of the most promising materials for the selective oxidation of methane to methanol. Data analysis points to a quasi-linear coordination geometry in the MOR side pocket and suggests that ca. 20% of the Cu-ions exist as coupled di-copper(I) species, paving the way for more detailed structural refinements.

Keywords

In situ XAS, DFT, Cu-mordenite, zeolites, methane-to-methanol

1. Introduction

The selective oxidation of methane to methanol (MTM) represents a *holy grail*, having the potential to revolutionize the energy sector and the chemical industry. Cu-exchanged zeolites are able to cleave the C-H bond of CH₄, stabilizing intermediate methyl species, which are released in the form of oxygenates (i.e. CH₃OH) upon interaction with H₂O (Ravi et al., 2017; Snyder et al., 2018). Depending on the zeolite topology, a number of active Cu-oxo species have been proposed to form during high-temperature activation in O₂ (Groothaert et al., 2005; Grundner et al., 2015; Pappas et al., 2017; Pappas et al., 2018; Sushkevich et al., 2017; Tsai et al., 2014; Vanelderen et al., 2015). However, the exact nature of the Cu active sites and the routes leading to their stabilization are still debated.

The unique structural/electronic sensitivity of X-ray absorption spectroscopy (XAS) assisted by Density Functional Theory (DFT) modelling has enabled remarkable advances in this direction (Bordiga et al., 2013; Borfecchia et al., 2018a; Borfecchia et al., 2015; Martini et al., 2017).

Cu-zeolites are known to undergo the so called ‘self-reduction’, yielding large populations of Cu(I) ions after thermal treatment in vacuum or inert gas flow (Borfecchia et al., 2015; Sushkevich and van Bokhoven, 2018; Turnes Palomino et al., 2000). In our previous work on Cu-chabazite, we showed how interaction of these Cu(I) ions with O₂ at 500 °C drives the material into a highly active state towards MTM (Pappas et al., 2017). Thus, a detailed characterization of the Cu(I) state represents a crucial starting point in investigating its reaction with O₂ to active-O₂/Cu(II) moieties relevant to the MTM conversion.

Herein, we apply DFT-assisted XAS analysis to investigate the local structure of Cu(I) ions in Cu-MOR, representing one of the most productive materials reported to date for MTM. The obtained results provide experimental support to previous proposals of quasi-linear Cu(I) species in the so-called MOR side pocket (Tsai et al., 2014; Vanelderen et al., 2015).

2. Materials and Methods

In situ XAS was collected on the BM23 beamline (Mathon et al., 2015) of the European Synchrotron Radiation Facility (ESRF, Grenoble, France) on a Cu-MOR zeolite (Cu/Al=0.36, Si/Al=11, Cu 3.18 wt%, as determined by EDS compositional analysis) synthesized as reported elsewhere (Borfecchia et al., 2018b). The material was prepared in the form of a self-supporting pellet of optimized mass and activated at 400 °C inside a devoted glass cell equipped with kapton windows, which allows to perform measurements under controlled atmosphere. After activation, the sample was cooled under vacuum and measured at room temperature (RT). Cu K-edge XAS spectra were collected in transmission mode, using a Si(111) double-crystal monochromator. The incident and transmitted X-ray intensities were detected using ionization chambers filled with a He/Ar mixture. To characterize the Cu(I)-MOR state, we collected four consecutive XAS scans in the 8800–9995 eV range (25 min/scan). After energy alignment and normalization to the edge-jump using Athena (Ravel and Newville, 2005), the four $\mu\text{x}(E)$ curves were averaged. The corresponding k^2 -weighted $\chi(k)$ function (Fig. 1b) was Fourier transformed (FT) in the $\Delta k = (2.4\text{--}12.0) \text{ \AA}^{-1}$ range.

The EXAFS fits were performed in R-space, in the $\Delta R = 1.0\text{--}5.0 \text{ \AA}$ range, using Artemis (Ravel and Newville, 2005). Phase and amplitude of each path were firstly calculated using as starting guess the DFT-optimized ZCu(I)@MOR_{SP} geometry (Fig. 2a). We included all the single scattering (SS) paths involving O and Al/Si atoms (referred to as O_{fw} and T_{fw}, respectively) in the investigated R range. To limit the number of optimized variables, all the included SS paths were optimized with the same amplitude factor (S_0^2) and energy shift (ΔE), both guessed in this initial fit. A subsequent fit included an additional Cu–Cu SS path, parametrized with fixed $\sigma_{\text{Cu}}^2 = 0.008 \text{ \AA}^2$ and guessed coordination number N_{Cu} . Here, S_0^2 was fixed to the best-fit value of 0.85 obtained in the first fit, to

avoid excessively high correlations with N_{Cu} . In both fits, the O/Si SS paths in the 3–5 Å range from the absorber were parametrized by a common contraction/expansion factor $\alpha_{\text{far-fw}}$ and a DW factor $\sigma_{\text{far-fw}}^2$ increasing as the square root of the path length R_{eff} (Borfecchia et al., 2015).

For DFT analysis, clusters of increasing sizes were extracted from the periodic structure of the MOR zeolite taken from the database of structures which is maintained by the IZA (Baerlocher and McCusker, 1996). Dangling bonds were saturated with hydrogen atoms at a bond length of 0.96 Å along the corresponding O-Si bonds of the crystal resulting in T-OH type clusters. One (or two) Si atom(s) at T3 site were replaced by Al leading to charged clusters. Si, O, and Al atoms in the 8 MR of the side pocket hosting the Al-substituted T sites and the Cu(I) ions were allowed to relax whereas the remaining atoms were kept fixed to maintain the rigidity of the crystalline zeolite. Convergence tests were performed for cluster size considering the adsorption energy of Cu(I) ions at the Al-substituted T sites (Fermann et al., 2005). These calculations converged for clusters with radii larger than 5 Å, containing at least 22 tetrahedral (Si or Al) atoms and showed a good agreement with the approach of designing zeolite clusters proposed by (Migues et al., 2015). All calculations have been carried out within Gaussian 09, Revision D. 01 (Frisch, 2016). Cu-MOR structures were optimized by the Kohn-Sham DFT (Kohn and Sham, 1965; Parr and Yang, 1994). DFT energies were determined using the Becke’s three-parameters hybrid exchange-correlation functional, B3LYP (Becke, 1993; Lee et al., 1988). For Cu(I) ions, Si, O and H atoms, the non-relativistic effective core potential (ECP) and LanL2DZ (Hay and Wadt, 1985) basis sets were used. Such basis sets are largely used to study molecules or clusters containing transition metals. Optimized geometries were characterized as minima (zero imaginary frequencies) evaluating the second-order derivative matrix from the vibrational analysis.

3. Results and discussion

Fig. 1 reports the *in situ* XAS data for the investigated Cu-MOR zeolite, after thermal treatment in vacuum at 400 °C and cooling to RT. From the XANES (Fig. 1a), it is clear that the Cu ions in the systems exist in a virtually pure Cu(I) oxidation state. Within the resolution of our measurements, no trace of the pre-edge peak arising from $1s \rightarrow 3d$ transition in d^9 Cu(II) ions is detected. The XANES is dominated by a prominent rising-edge peak at 8982.5 eV, assigned to the $1s \rightarrow 4p$ transition in Cu(I) ions. The rising-edge peak is only slightly less intense than the white-line peak at 8994.5 eV. Overall, the XANES for Cu(I)-MOR closely resembles the one of the linear $[\text{Cu(I)(NH}_3)_2]^+$ model compound (Giordanino et al., 2014; Janssens et al., 2015). In line with previous Cu K-edge XANES studies (Kau et al., 1987; Solomon et al., 2014), the characteristic XANES features observed here point to quasi-linear Cu(I) sites. Notably, similar XANES features are detected under *operando* conditions during the MTM process over Cu-MOR, after interaction of CH_4 with the O_2 -activated materials (Borfecchia et al., 2018b).

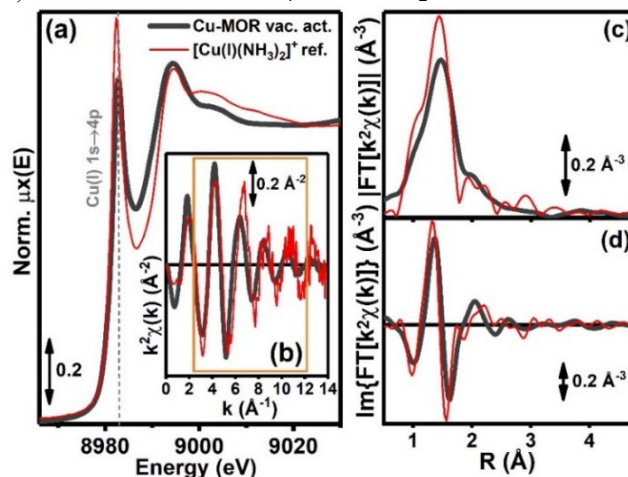


Fig. 1. (a) *In situ* Cu K-edge XANES of the investigated Cu(I)-MOR zeolite obtained after activation at 400 °C in vacuum compared with the XANES of the perfectly linear $[\text{Cu(I)(NH}_3)_2]^+$ model compound (Janssens et al., 2015). (b) Correspondent $k^2\chi(k)$ EXAFS spectra; the k-range employed for the FT (2.4-12.0 Å⁻¹) is highlighted by an orange box. (c, d) Phase-uncorrected (c) modulus and (d) imaginary part of the FT-EXAFS spectra of Cu(I)-MOR and $[\text{Cu(I)(NH}_3)_2]^+$.

In the phase-uncorrected FT-EXAFS, we note a first maximum at 1.5 Å, with a broad shoulder at 2.1 Å. At longer R-values, only a broad feature peaking at 3.9 Å is observed. The first shell intensity is compatible with the one observed for the $[\text{Cu(I)(NH}_3)_2]^+$ model compound, suggesting the presence of two framework O atoms ($\text{O}_{1\text{fw}}$) in the first coordination shell of Cu. To get further insights in the local structure of Cu(I) ions, we turned to DFT-assisted EXAFS analysis. Here, computational analysis is employed as a guide in defining the absorber local environment, i.e. number/type of coordination shells and related coordination numbers (Borfecchia et al., 2015), avoiding excessively high correlations among fitting parameters. Driven by previous studies on Cu(I) in the MFI (Tsai et al., 2014) and MOR (Vanelderen et al., 2015) frameworks, we explored the coordination of Cu(I) inside

the side-pocket (SP) of the MOR zeolite. By DFT, we considered both a monomeric Cu(I) site (Fig. 2a) and a coupled Cu(I)⋯Cu(I) site (Fig. 2b). In both cases, DFT confirms a quasi-linear geometry for Cu(I) sites, coordinated to two O_{1fw} atoms with bond angles of about 144°. The second-shell environment is composed by an additional O_{2fw} atom and, at slightly longer distances, a Si atom and the charge-balancing Al one. For the coupled Cu(I)⋯Cu(I) model, DFT indicates a Cu–Cu distance of 3.57 Å.

Initially, we fitted the experimental spectrum of Cu(I)-MOR using the ZCu(I) @MOR_{SP} model as starting input (Fig. 2c,d). Overall, the model provided a good reproduction of the experimental data up to 3.5 Å, with an R-factor value < 1% and physically meaningful values of all the optimized parameters (Table 1).

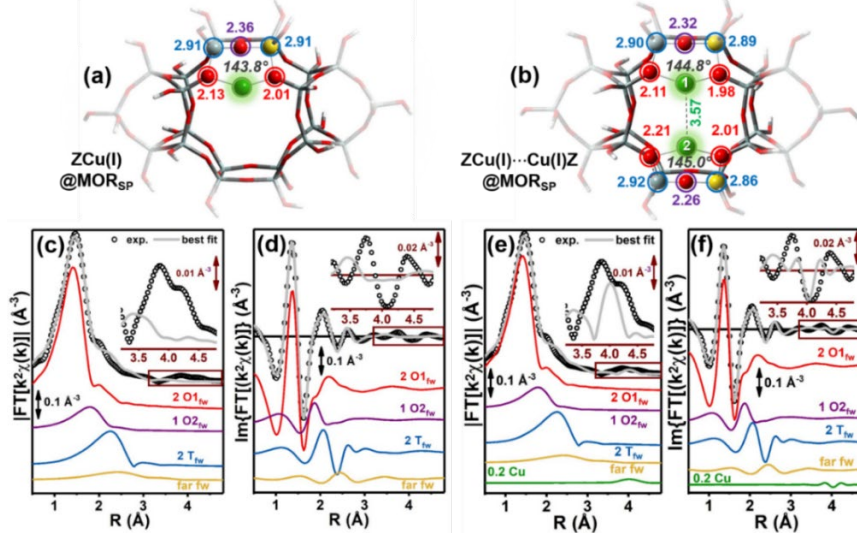


Fig. 2. (a) DFT-optimized model of ZCu(I)@MOR_{SP} (Cu, green; O, red; Si, grey; Al, yellow). DFT distances from the Cu center (Å) and O_{1fw}CuO_{1fw} bond angles (°) are indicated. (b) The same as part (a) but for ZCu(I)⋯Cu(I)@MOR_{SP}. (c, d) Comparison between experimental and best fit FT-EXAFS spectra (magnitude and imaginary parts in parts (c) and (d), respectively) using the ZCu(I)@MOR_{SP} as initial guess. The principal contributions to the EXAFS signal are also reported, vertically translated for clarity. (e, f) The same as parts (c, d) but adding a Cu-Cu SS path in the fit model.

Table 1. Best-fit parameters optimized in the EXAFS fit of the k²-weighted spectra of Cu(I)-MOR.

Fit parameters	ZCu(I) @MOR _{SP}		ZCu(I)⋯Cu(I)Z @MOR _{SP}	
	DFT	EXAFS	DFT	EXAFS
S ₀ ²		0.85 ± 0.05		<u>0.85</u>
ΔE (eV)		− 5 ± 1		− 5 ± 1
Fit R-factor		0.00836		0.00768
n° par. (n° ind.)		10 (26)		11 (26)
N _{O1fw}		<u>2</u>		<u>2</u>
<R _{O1fw} > (Å)	2.07	1.923 ± 0.002	2.05/2.11 ^a	1.923 ± 0.002
σ ² _{O1fw} (Å ²)		0.0038 ± 0.0004		0.0038 ± 0.0004
N _{O2fw}		<u>1</u>		<u>1</u>
R _{O2fw} (Å)	2.36	2.39 ± 0.01	2.32/2.26 ^a	2.39 ± 0.01
σ ² _{O2fw} (Å ²)		0.015 ± 0.002		0.013 ± 0.002
N _{Tfw}		<u>2</u>		<u>2</u>
<R _{Tfw} > (Å)	2.91	2.93 ± 0.01	2.90/2.89 ^a	2.93 ± 0.01
σ ² _{Tfw} (Å ²)		0.016 ± 0.002		0.015 ± 0.003
N _{Cu}		–		0.2 ± 0.1
R _{Cu} (Å)	–	–	3.57	4.37 ± 0.05
σ ² _{Cu} (Å ²)		–		<u>0.008 ± 0.002</u>
α _{far-fw}		− 0.05 ± 0.01		− 0.05 ± 0.01
σ ² _{far-fw} (Å ²)		0.02 ± 0.01		0.02 ± 0.01

^a Values for sites 1 and 2, respectively (see ZCu(I)⋯Cu(I)Z@MOR_{SP} geometry in Fig. 2b).

The EXAFS-optimized Cu–O_{1fw} bond length is ~ 0.15 Å shorter than the DFT one, while the other are structural parameters are globally in fair agreement with the optimized geometry. Nonetheless, the high DWs values

obtained for the O_{2fw} and T_{fw} contributions evidence a high level of structural disorder in the second coordination sphere of Cu(I) ions. Fitting results allow us to rationalize the absence of a well-defined second-shell peak with the partial antiphase between SS involving the O_{2fw} and T_{fw} atoms, together with small but significant structural differences among Cu(I) species hosted at different Al sites in the zeolite. Nonetheless, the broad EXAFS feature centred at ca. 3.9 Å in the experimental spectrum was not reproduced by the $ZCu(I)@MOR_{SP}$ model (insets of Fig. 2c,d).

DFT results show how the same coordination mode is still kept for both mono-copper and coupled di-copper sites. Thus, we have repeated the fit including an additional Cu–Cu SS path to assess the presence and the abundance of $ZCu(I)\cdots Cu(I)Z$ cores (Fig. 2e,f). While the best-fit EXAFS parameters remained largely unchanged with respect to the initial fit (Table 1), the additional Cu–Cu contribution allowed us to significantly improve the signal reproduction in the high-R range (insets of Fig. 2e,f). EXAFS analysis suggests that 20 ± 10 % of Cu ions in the system participate into such *coupled* configurations. However, the Cu–Cu distance refined from EXAFS, 4.37 ± 0.05 Å, significantly exceeds the one predicted by DFT. It is clear that experimental peak we are attempting to reproduce consists in a broad feature, most likely reflecting a broad distribution of Cu–Cu distances, depending on Al siting in the zeolite lattice as well as on the higher mobility of Cu(I) ions with respect to Cu(II) ones (Görtl et al., 2016). Overall, the proposed models resulted in a satisfactory but preliminary fit to the data, paving the way to future work needed to fully reproduce the experimental signal.

4. Conclusions

In this work we combined *in situ* XAS and computational modelling to characterize the local structure of Cu(I) ions in the MOR zeolite. The characteristic XANES features suggest quasi-linear Cu(I) species coordinated to two framework oxygens. DFT optimization of mono-copper(I) and *coupled* di-copper(I) species in the MOR side pocket confirms the qualitative insights from XANES. DFT-assisted EXAFS fits further corroborated the local structure of Cu(I) species. EXAFS analysis evidenced a quite high level of structural disorder from the second coordination sphere of the cations, as well as the presence of long-range Cu–Cu contributions involving ca. 20% of the Cu ions. These results represent the first step towards a more detailed structural analysis of Cu(I) ions in the MOR framework. Moreover, the obtained insights will pave the way to future computational/spectroscopic studies targeting to the interaction of O_2 with the Cu(I) species characterized here, of relevance in designing selective oxidation processes for the valorisation of the lowest alkanes.

References

- Baerlocher, C., McCusker, L.B., 1996. Database of Zeolite Structures, <http://www.iza-structure.org/databases/>. International Zeolite Association.
- Becke, A.D., 1993. J. Chem. Phys. 98, 5648-5652.
- Bordiga, S., Groppo, E., Agostini, G., van Bokhoven, J.A., Lamberti, C., 2013. Chem. Rev. 113, 1736-1850.
- Borfecchia, E., Beato, P., Svelle, S., Olsbye, U., Lamberti, C., Bordiga, S., 2018a. Chem. Soc. Rev. doi: 10.1039/C8CS00373D.
- Borfecchia, E., Lomachenko, K.A., Giordanino, F., Falsig, H., Beato, P., Soldatov, A.V., Bordiga, S., Lamberti, C., 2015. Chem. Sci. 6, 548-563.
- Borfecchia, E., Pappas, D.K., Dyballa, M., Lomachenko, K.A., Negri, C., Signorile, M., Berlier, G., 2018b. Catal. Today doi: 10.1016/j.cattod.2018.07.028.
- Fermann, J.T., Moniz, T., Kiowski, O., McIntire, T.J., Auerbach, S.M., Vreven, T., Frisch, M.J., 2005. J. Chem. Theory Comput. 1, 1232-1239.
- Frisch, M.J., 2016. Gaussian 09, Revision D 01. Gaussian, Inc., Wallingford CT.
- Giordanino, F., Borfecchia, E., Lomachenko, K.A., Lazzarini, A., Agostini, G., Gallo, E., Soldatov, A.V., Beato, P., Bordiga, S., Lamberti, C., 2014. J. Phys. Chem. Lett. 5, 1552-1559.
- Görtl, F., Sautet, P., Hermans, I., 2016. Catal. Today 267, 41-46.
- Groothaert, M.H., Smeets, P.J., Sels, B.F., Jacobs, P.A., Schoonheydt, R.A., 2005. J. Am. Chem. Soc. 127, 1394-1395.
- Grundner, S., Markovits, M.A., Li, G., Tromp, M., Pidko, E.A., Hensen, E.J., Jentys, A., Sanchez-Sanchez, M., Lercher, J.A., 2015. Nat. Commun. 6, 7546.
- Hay, P.J., Wadt, W.R., 1985. J. Chem. Phys. 82, 270-283.
- Janssens, T.V.W., Falsig, H., Lundegaard, L.F., Vennestrøm, P.N.R., Rasmussen, S.B., Moses, P.G., Giordanino, F., Borfecchia, E., Lomachenko, K.A., Lamberti, C., Bordiga, S., Godiksen, A., Mossin, S., Beato, P., 2015. ACS Catal. 5, 2832-2845.
- Kau, L.S., Spirasolomon, D.J., Pennerhahn, J.E., Hodgson, K.O., Solomon, E.I., 1987. J. Am. Chem. Soc. 109, 6433-6442.
- Kohn, W., Sham, L.J., 1965. Phys. Rev. 140, A1133-A1138.
- Lee, C., Yang, W., Parr, R.G., 1988. Phys. Rev. B 37, 785-789.
- Martini, A., Borfecchia, E., Lomachenko, K.A., Pankin, I.A., Negri, C., Berlier, G., Beato, P., Falsig, H., Bordiga, S., Lamberti, C., 2017. Chem. Sci. 8, 6836-6851.

Mathon, O., Beteva, A., Borrel, J., Bugnazet, D., Gatla, S., Hino, R., Kantor, I., Mairs, T., Munoz, M., Pasternak, S., Perrin, F., Pascarelli, S., 2015. *J. Synchrot. Radiat.* 22, 1548-1554.

Migues, A.N., Muskat, A., Auerbach, S.M., Sherman, W., Vaitheeswaran, S., 2015. *ACS Catal.* 5, 2859-2865.

Pappas, D.K., Borfecchia, E., Dyballa, M., Pankin, I.A., Lomachenko, K.A., Martini, A., Signorile, M., Teketel, S., Arstad, B., Berlier, G., Lamberti, C., Bordiga, S., Olsbye, U., Lillerud, K.P., Svelle, S., Beato, P., 2017. *J. Am. Chem. Soc.* 139, 14961-14975.

Pappas, D.K., Martini, A., Dyballa, M., Kvande, K., Teketel, S., Lomachenko, K.A., Baran, R., Glatzel, P., Arstad, B., Berlier, G., Lamberti, C., Bordiga, S., Olsbye, U., Svelle, S., Beato, P., Borfecchia, E., 2018. *J. Am. Chem. Soc.* 140, 15270-15278.

Parr, R.G., Yang, W., 1994. *Density-Functional Theory of Atoms and Molecules*. Oxford University Press.

Ravel, B., Newville, M., 2005. *J. Synchrotron Radiat.* 12, 537-541.

Ravi, M., Ranocchiari, M., van Bokhoven, J.A., 2017. *Angew. Chem. Int. Edit.* 56, 16464-16483.

Snyder, B.E.R., Bols, M.L., Schoonheydt, R.A., Sels, B.F., Solomon, E.I., 2018. *Chem. Rev.* 118, 2718-2768.

Solomon, E.I., Heppner, D.E., Johnston, E.M., Ginsbach, J.W., Cirera, J., Qayyum, M., Kieber-Emmons, M.T., Kjaergaard, C.H., Hadt, R.G., Tian, L., 2014. *Chem. Rev.* 114, 3659-3853.

Sushkevich, V.L., Palagin, D., Ranocchiari, M., van Bokhoven, J.A., 2017. *Science* 356, 523-527.

Sushkevich, V.L., van Bokhoven, J.A., 2018. *Chem. Commun.* 54, 7447-7450.

Tsai, M.L., Hadt, R.G., Vanelderen, P., Sels, B.F., Schoonheydt, R.A., Solomon, E.I., 2014. *J. Am. Chem. Soc.* 136, 3522-3529.

Turnes Palomino, G., Fisticaro, P., Bordiga, S., Zecchina, A., Giamello, E., Lamberti, C., 2000. *J. Phys. Chem. B* 104, 4064-4073.

Vanelderen, P., Snyder, B.E., Tsai, M.L., Hadt, R.G., Vancauwenbergh, J., Coussens, O., Schoonheydt, R.A., Sels, B.F., Solomon, E.I., 2015. *J. Am. Chem. Soc.* 137, 6383-6392.

Acknowledgments. CB, KK and DKP acknowledge financial support from the Research Council of Norway under contract n. 237922 (iCSI industrial Catalysis Science and Innovation Centre) and contract n. 250795 (CONFINE project). EB acknowledges Innovation Fund Denmark (Industrial postdoc n. 5190-00018B). IAP and AM acknowledge the Ministry of Education and Science of the Russian Federation for the award of Grant n. 16.3871.2017/4.6 ("Picometre diagnostics of parameters of 3D atomic structure of nanomaterials on the basis of XANES spectroscopy"). We are grateful to G. Berlier, S. Bordiga, C. Lamberti (University of Turin); M. Dyballa, S. Svelle, U. Olsbye, K. P. Lillerud (University of Oslo) and P. Beato (Haldor Topsøe A/S) for insightful discussion and advices.